Optimization of a photovoltaic pumping system in Bejaia (Algeria) climate

K. Rahrah, D. Rekioua, T. Rekioua
Laboratoire LTII, Universite de Bejaia (Algeria)
dja_rekioua@yahoo.fr

Abstract: *Photovoltaic energy is used in different applications and especially in water pumping and irrigation in remote areas. However, the performances of a photovoltaic pumping system can be degraded with variations of insolation and in order to maximize the efficiency of the photovoltaic energy system, it is necessary to track the maximum power point of the PV array. Many methods have been developed to determine the maximum power point (MPP). In this paper we present the results of performance optimization of a PV pumping system in Bejaia (Algeria) climate. The pumped water is desired to satisfy the domestic needs of three different families during three consecutive years (2004-2006). The proposed system is presented. It consists of PV arrays, a motor-pump, and a maximum power point tracker. Due to the intermittent nature of photovoltaic energy source, batteries are added for the purpose of ensuring continuous power flow. The storage battery model used is presented with obtained measurement results. Simulation is developed under Matlab-Simulink Package. Some experimental results are also given to show the effectiveness of the studied system.*

Keywords: *Photovoltaic systems, Pumping, Maximum power point tracker, simulation, Storage battery.*

I. INTRODUCTION

Solar energy which is free and abundant in most parts of the world has proven to be an economical source of energy in many applications. Algeria receives large quantities of solar radiations all over the year and PV pumping is clearly the solution to the water problem in remote sites. Actually, in Algeria, the number of photovoltaic energy-driven water pumps is very low. The main obstacles to the PV pumping development and dissemination are the high initial investment, the low awareness about these systems and the lack of tools serving to predict their performances. The climate varies from the Mediterranean type in the north to the desert type in the south. Algeria with a total area of 2,381,741 km^2, can be divided into three climatic regions which run parallel to each other horizontally through the country.

We present in this paper the results of performance optimization of a PV pumping system in Bejaia (Algeria) climate. The pumped water is desired to satisfy the domestic needs of three different families during three consecutive years (2004-2006). The proposed system consists of PV arrays, AC motor, centrifugal pump, a storage tank and a maximum power point tracker. The paper is organized as follows. In Section II, we present the photovoltaic pumping system with battery storage used. Mathematical relations between the essential variables of a PV system are presented in Section III. These relations are necessary for simulating its operation under different irradiance and temperature levels. Due to the intermittent nature of photovoltaic energy source, batteries are added for the purpose of ensuring continuous power flow. The storage battery model used is presented with obtained measurement results. The control system is required to track maximum power whatever environmental conditions variations. In Section IV, an MPPT method is developed in order to track the MPP of a PV system. Simulated results, achieved using the MATLAB®-SIMULINK® package, based on climatic data, are given in Section V. Finally, Section VI concludes the work.

II. SYSTEM DESCRIPTION

A. Description :

A general photovoltaic pumping system consists of PV arrays, a boost chopper working as a maximum power point tracker (MPPT), an inverter and a motor driving a pump.

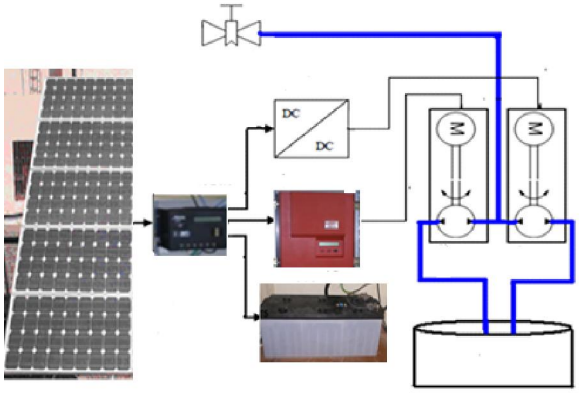

Fig.1 System description

B. Modeling of photovoltaic generator

In literature, there are several mathematical models that describe the operation and behavior of the photovoltaic generator [4]. These models differ in the calculation procedure, accuracy and the number of parameters involved in the calculation of the current-voltage characteristic.

B.1First model:

The simplest model of a PV cell is shown as an equivalent circuit below that consists of an ideal current source in parallel with an ideal diode. The current source represents the current generated by photons, and its output is constant under constant temperature and constant incident radiation of light. The model is called one diode and the equivalent circuit (Fig 2) consists of a single diode for the cell polarization phenomena and two resistors (series and shunt) for the losses.

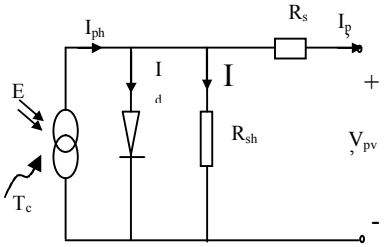

Fig 2.Simplified equivalent circuit of solar cell

I(V) characteristic of this model is given by the following equation [5]:

$$I_{pv} = I_{ph} - I_d - I_{Rsh} \quad (1)$$

$$I_{pv} = I_{ph} - I_0\left[e^{q\frac{(V_{pv}+I_{pv}.R_s)}{AkT_j}} - 1\right] - \frac{V_{pv}}{R_{sh}} \quad (2)$$

The photocurrent, I_{ph}, is directly dependent upon both insolation and panel temperature, and may be written in the following form:

$$I_{ph} = P_1.E.\left[1 + P_2.(E - E_{ref}) + P_3.(T_j - T_{ref})\right] \quad (3)$$

Where*: E* insolation in the panel plane (W/m²); E_{ref} corresponds to the reference insolation of 1000 W/m² and T_{jref} to the reference panel temperature of 25°C. P_1, P_2 and P_3 are constant parameters.

The polarization current I_d of junction PN, is given by the expression:

$$I_d = I_0.[\exp(\frac{q.(V_{pv} + R_s.I_{pv})}{A.n_s.k.T_j}) - 1] \quad (4)$$

With:

I_0 (A) saturation current, q the elementary charge (ev), k Botzman's constant, A ideality factor of the junction, T_j : junction temperature of the panels (°K) and R_s, R_{sh} (Ω) resistors (series and shunt).

B.2 Second Model

The PV array equivalent circuit current I_{pv} can be expressed as a function of the PV array voltage V_{pv}:

$$I_{pv} = I_{sc}\left\{1 - C_1\left[\exp\left(C_2 V_{pv}^{m}\right) - 1\right]\right\} \quad (5)$$

Where the coefficients C_1, C_2 and m are defined as:

$$C_1 = 0.01175 \quad (6)$$

$$C_2 = \frac{C_4}{V_{oc}^{m}} \quad (7)$$

$$C_3 = \ln\left[\frac{I_{sc}(1 + C_1) - I_{mpp}}{C_1 I_{sc}}\right] \quad (8)$$

$$C_4 = \ln\left[\frac{1 + C_1}{C_1}\right] \quad (9)$$

$$m = \frac{\ln\left[\frac{C_3}{C_4}\right]}{\ln\left[\frac{V_{mpp}}{V_{oc}}\right]} \quad (10)$$

Where: V_{mpp} voltage at maximum power point; V_{oc} open circuit voltage; I_{mpp} current at maximum power point; I_{sc} short circuit current.

Equation (5) is only applicable at one particular insolation level E, and cell temperature, T_J, at standard test conditions (STC) (E=1000 W/m², T_j=25 °C). When insolation and temperature vary, the parameters change according to the following equations:

$$\Delta T_j = T_j - T_{jref} \quad (11)$$

$$\Delta I_{pv} = \alpha_{sc}\left(\frac{E}{E_{ref}}\right)\Delta T_j + \left(\frac{E}{E_{ref}} - 1\right)I_{sc,ref} \quad (12)$$

$$\Delta V_{pv} = -\beta_{oc}\Delta T_j - R_s\Delta I_{pv} \quad (13)$$

The new values of the photovoltaic voltage and the current are given by:

$$V_{pv,new} = V_{STC} + \Delta V_{pv} \quad (14)$$

$$I_{pv,new} = I_{STC} + \Delta I_{pv} \quad (15)$$

B.3 Third model

In the model "two diodes", the two diodes are present for the PN junction polarization phenomena. These diodes represent the recombination of the minority carriers, which are located both at the surface of the material and within the volume of the material (Fig.3.).

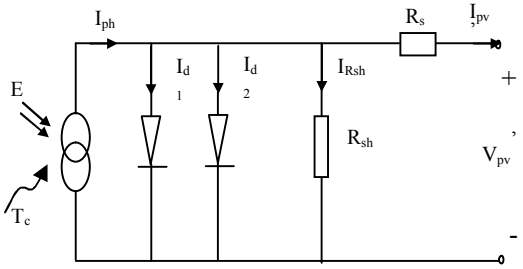

Fig.3 Equivalent circuit for two diode model

The following equation is then obtained:

$$I_{pv} = I_{ph} - (I_{d2} + I_{d2}) - I_{Rsh} \quad (16)$$

with I_{ph} and I_{Rsh} maintaining the same expressions as above. For the recombination currents:

$$I_{d1} = I_{01}\left[\exp(\frac{q.(V_{pv} + R_S.I_{pv})}{A.n_s.k.T_j}) - 1\right] \quad (17)$$

$$I_{d2} = I_{02}\left[\exp(\frac{q.(V_{pv} + R_S.I_{pv})}{2.A.n_s.k.T_j}) - 1\right] \quad (18)$$

The saturation currents then become:

$$I_{01} = P_{04}.T_j^{3}.\exp\left(\frac{-E_g}{k.T_j}\right) \quad (19)$$

$$I_{02} = P_{14}.T_j^{3}.\exp\left(\frac{-E_g}{2.k.T_j}\right)$$

The final equation of the model is thereby written as:

$$I_{pv} = P_1.E.\left[1 + P_2.(E - E_{ref}) + P_3.(T_j - T_{ref})\right] - \frac{(V_{pv} + R_s.I_{pv})}{R_{sh}}$$
$$- P_{04}.T_j^{3}.\exp\left(\frac{-E_g}{k.T_j}\right).\left[\exp\left(q.\frac{V_{pv} + R_s.I_{pv}}{A.n_s.k.T_j}\right) - 1\right] \quad (20)$$
$$- P_{14}.T_j^{3}.\exp\left(\frac{-E_g}{2.k.T_j}\right).\left[\exp\left(q.\frac{V_{pv} + R_s.I_{pv}}{2.A.n_s.k.T_j}\right) - 1\right]$$

With a total of 8 parameters (P_1, P_2, P_3, P_4, P_5, A, R_s and R_{sh}) to be determined.

Figure 4 show the current/voltage characteristics obtained using the three models compared with the experimental values corresponding to a 110 Wc Siemens panel (Table 1.)

TABLE.1
Parameter of the PV panel SIEMENS SM 110-24

P_{PV}	110W
I_{mpp}	3.15A
V_{mpp}	35V
I_{sc}	3.45A
V_{oc}	43.5V
α_{sc}	1.4mA/°C
β_{oc}	-152mV/°C
P_{mpp}	110W

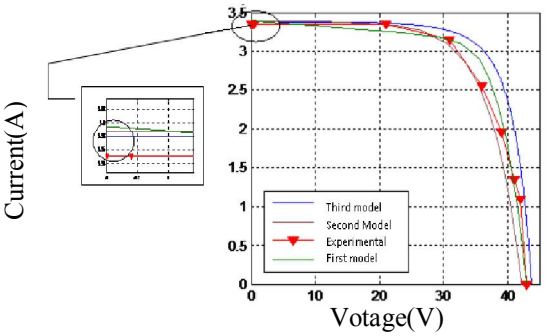

Fig 4. I(V) characteristics of 110 Wc Pannel.

A calculation error was made. We note that the third model (with two diodes) is the most accurate model with an error committed of 0.89% (Fig. 5).

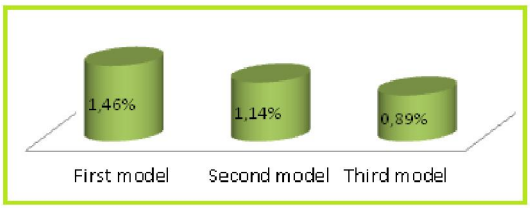

Fig 5. Calculation error

C. *Modeling subsystem pumping*

A motor-pump consists of a centrifugal pump coupled with a three-phase induction machine. Several types of DC and AC motors are available for PV pumping systems. The choice of the motor is dependent on numerous factors including size requirement, efficiency, price, reliability and availability.
Generally, the PV water pumping system needs a water tank for storing water. If there is no water tank or the system is used as potable equipment, the battery set will be necessary.

C.1 Pump model
Many different varieties of pumps are used with PV-pumping system. In our case, a centrifugal pump is considered. This type of pump is simple and requires minimum maintenance. In our case, we use the model expresses the water flow output (Q) directly as a function of the electrical power input (P) to the motor-pump, for different total heads. A polynomial fit of the third order expresses the relationship between the flow rate and power input, as described by the following equation [6, 7]:

$$P(Q,h) = a(h)Q^3 + b(h)Q^2 + c(h)Q + d(h) \quad (21)$$

Where:P is the electrical power input of the motor-pump, h is the total head and a(h), b(h), c(h), d(h) are the coefficients corresponding to the working total head.

$$a(h) = a_0 + a_1h^1 + a_2h^2 + a_3h^3 \quad (22)$$

$$b(h) = b_0 + b_1h^1 + b_2h^2 + b_3h^3 \quad (23)$$

$$c(h) = c_0 + c_1h^1 + c_2h^2 + c_3h^3 \quad (24)$$

$$d(h) = d_0 + d_1h^1 + d_2h^2 + d_3h^3 \quad (25)$$

With ai, bi, and di it: constants and only depend on the type of sub-solar pumping system.
The calculation of the instantaneous flow in terms of power is calculated using Newton-Raphson method. Thus at the kth iteration, the flow Q is given by the following equation:
For $d - Pa(Q) > 0$:

$$Q_k = Q_{k-1} - \frac{F(Q_{k-1})}{F'(Q_{k-1})} \quad (26)$$

With: $F(Q_{k-1}) = a Q^3_{k-1} + b Q^2_{k-1} + c Q_{k-1} + d - P_a(Q_{k-1})$
Where:$F'(Q_{k-1})$ is the derivative of the function $F(Q_{k-1})$

D. Controller
In PV water pumping systems, the maximum power point tracking (MPPT) is usually used as a control strategy to track the maximum output power operating point of the photovoltaic generator for different operating conditions of insolation and temperature.
The main component of the MPPT is the DC-DC converter that steps down the solar panel output voltage to the desired load voltage. The DC-DC converter is used to increase the efficiency of the system by matching the voltage supplied to the voltage required by the load. It can be either be a Buck, a Boost or a Buck-Boost converter.
The MPPT is necessary to draw the maximum amount of power from the PV module. In our work, we use the Perturb and Observ (P&O) algorithm. In this strategy, the voltage is perturbed by a small increment and the resulting change in power is observed. If the change in power is positive, the voltage is adjusted by the same increment and the power is again observed. It continuous until the change in power is negative.

E. Battery bank.
We opted for the CIEMAT model. It is characterized by setting a series of women with a variable resistor (Fig.6). The characteristics of the source voltage Eb and internal resistance Rb depend on temperature and battery charge state.
For a number nb of cell, voltage equation is:

$$V_{batt} = n_{batt}.E_{batt} \pm n_{batt}.R_{batt}.I_{batt} \quad (27)$$

With : V_{batt}: battery voltage, I_{batt}: battery current., E_{batt}: electromotive force depending on the battery charge state., R_{batt}: internal resistance which varies with the state of charge.

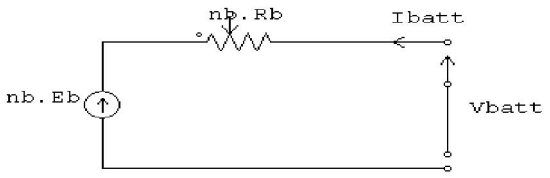

Fig.6 Equivalent circuit model CIEMAT

We use lead acid batteries of 12V, 92Ah. A measurement system was developed (Fig.7). We close the battery on a circuit including a rheostat of the current limitation (15.8Ω, 10A), a shunt (250V, 10A) allowing to measure the circulating current in the circuit and a source of alternating voltage (0-36V, 20A).

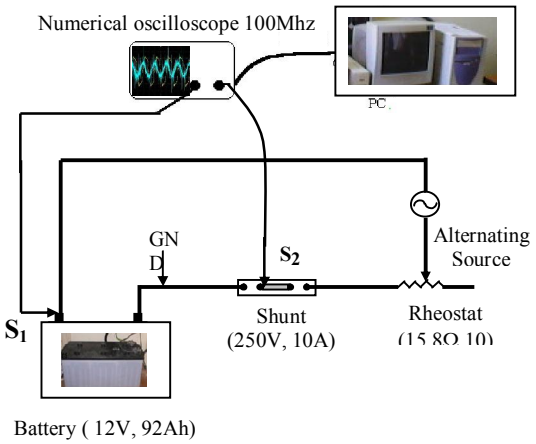

Battery (12V, 92Ah)

Fig.7. Circuit measurement of battery impedances.

Measures of the two signals are carried out by a numerical oscilloscope 100MHz with double track, model OX 8627, that makes the acquisition of signals possible, then to transfer them to a computer for analysis. The first signal is at the shunt boundaries which is a direct image of the current circulating in the circuit and the second one at the battery boundaries. The ratio of these two voltages and their dephasing provides the absolute value of the internal impedance of the battery Fig.8 presents measured signals S_1 and S_2 (conversion factor: 50V=1A)

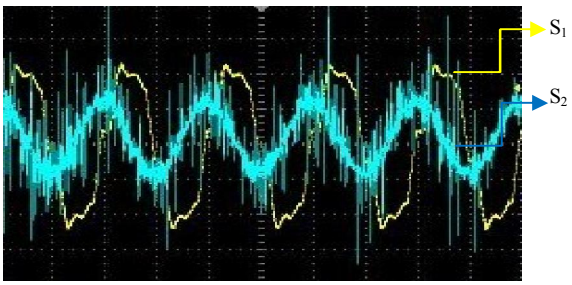

Fig 8 Measured signals S_1: current and S_2: Voltage.

The battery behaves as complex impedance Z_{batt} containing a resistance R_{batt} and a reactance X_{batt} to this disturbance.

$$Z_{batt} = R_{batt} - jX_{batt} \quad (28)$$

The module of the complex impedance is thus well defined by the ratio of the absolute values of the two signals. We deduce the dephasing by the temporal difference between the two signals with the passage by zero.

$$|Z_{batt}| = V_{batt} / I_{batt}$$

Knowing the module of Z_{batt} and dephasing. We can thus deduce the real part R_{batt} and imaginary X_{batt} of the impedance for his state of charge, these values changes according to the latter. We obtain:

R_{batt}	X_{batt}	C_{batt}
0.577Ω	0.15Ω	21.22mF

We give some simulations results

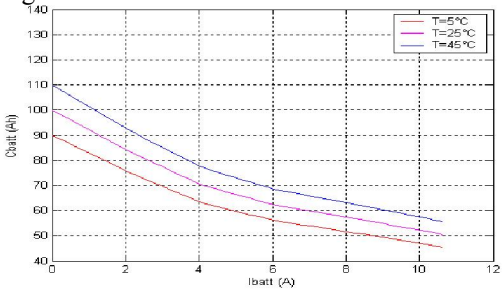

Fig9.Variation of the battery capacity for different temperatures

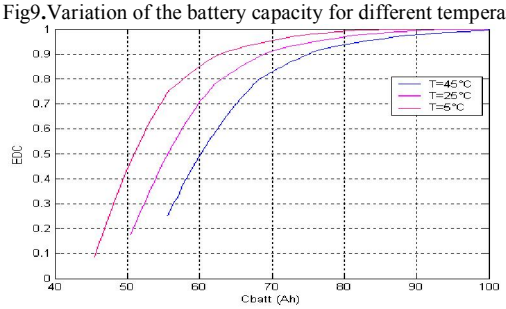

Fig 10 Variation of state of charge according to capacity battery for different temperatures

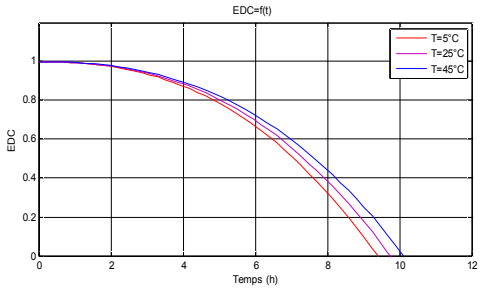

Fig 11. Varaions of state charge according to time of discharge for different temperatures

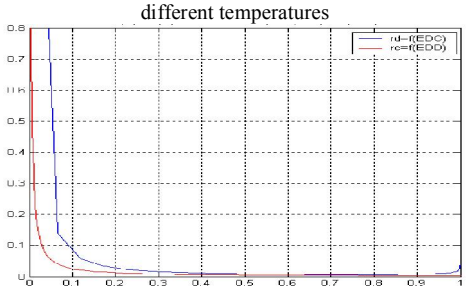

Fig 12. Variation of load voltage and the discharge based on EDD and EDC

III WATER NEEDS IN ALGERIA

Algeria climate can be considered as arid or at least as semi arid over the major part of the country. Thus, limited renewable surface and ground water resources are available. The water requirements are expected to increase because of the population growth, extension of irrigated area and industrial development.

The determination of water needs for consumption of a given population depends mainly on lifestyle, environment and climate of each region to assess needs of drinking water to urban and suburban Algerian families, we collected Data on the consumption of drinking water for three profiles.

- Profile N°1 Urban Family(PF1):
- Profile N°2 Urban Family (PF2):
- Profiel N° 3 Suburban family (PF3):

Data to be displayed in the following are collected from the discharge of potable water consumption of the three profils, as well as those given by the company producing and distributing Water Bejaia.

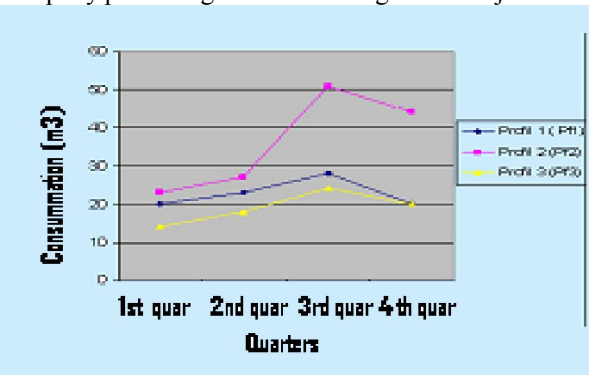

Fig13. Consummation drinking water each quarter during 2004

Note that the shape of the curve of the consumption of drinking water is the same for the three (03) profiles. It is important during the third quarter (July-August-September), and lowest during the first quarter (January-February-March). We also note that the water needs for consummation differ from profile to another, that mainly depends on the life style.

Figure 14 shows the variation of the consumption of drinking water for the 03 profiles from 2004 to 2006. Note that consumption is not stable but it changes from one year to another. We note from Figure 15 that the cost varies depending on consummation

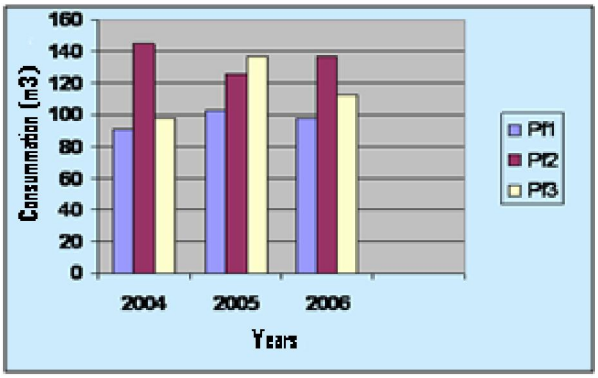

Fig.14. Consummation of drinking water during the years 2004, 2005 and 2006

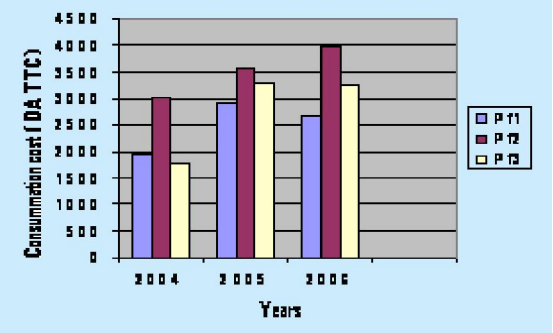

Fig.15 Cost of Consummation of drinking water during 2004, 2005 and 2006

E. Sizing the PV generator:

To size the PV array is defined data on average monthly sunshine with an inclination of the field equal to Bejaia latitude (36.43 ° N) for one year of operation and operating temperature. It is possible to represent the shape of the curves corresponding to changes in the sun at different settings for a day. Figure 16 shows the variation of insolation measured in Bejaia on an incline of 45 degrees towards the south, from 8h to 18h for different days (spring, summer and winter).

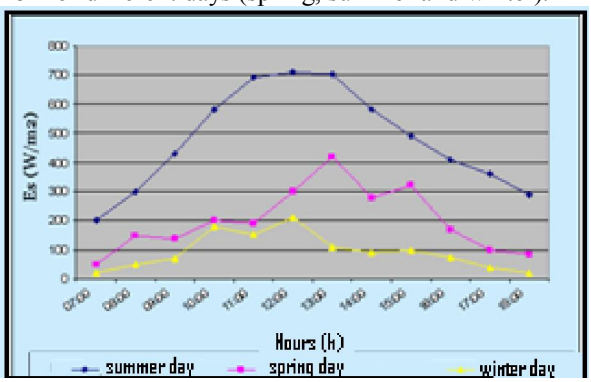

Fig.16 Change in the Sunshine Es for different periods

We note that the shape of the curve of the variation of insolation during a summer day is in the form of a bell has a maximum of about 710 W / m² to 12: 30.

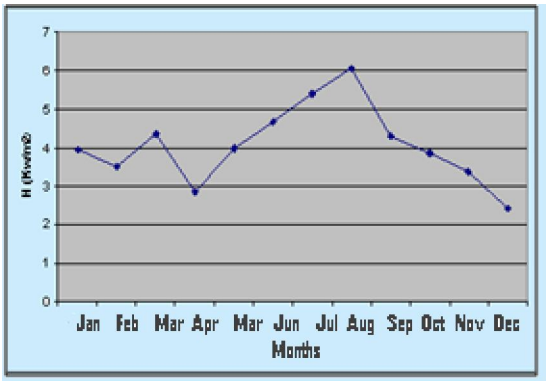

Fig.17 Variation of average sunshine during 2007

II.SIMULATION SYSTEM FOR PUMPING

Based on recent models, a simulation program of pumping systems has been developed for the calculation of electrical performance, hydraulic pumping systems. This program simulates the

operation of pumping systems based on several parameters such as: height gauge, the solar irradiance and solar power generator. The performance of pumping systems are calculated using a PV generator 550Wc with a configuration of a branch of SIEMENS MS 5 modules in series 24V 110W (5S x 1p). This generator feeds both subsystems pumping SP1 or SP2: SP1. The first system consists of a DC motor and a pump progressive cavity. The second system consists of SP2 is a three phase AC motor and a multistage centrifugal pump. The results simulation performance daily, depending on annual weather data logic Bejaia is presented in figures (18, 19 and 20).

We comment on the figures (18 and 19) the volume of water pumped by two systems is important during the summer and lowest during the winter. The latter is due to the variation of solar radiation is also higher in summer than in spring and winter. The varying amount of water pumped by both SP1 and SP2 systems during 2007 is illustrated in Figure 20 shows that the flow is greatest during the months (June, July, August) and minimum during the month of December. We also note that the quantity of water pumped by the SP1 is more important than that pumped by SP2.

III. CONCLUSION

In this work, we have simulated the operation of pumping systems for drinking water supply. The analysis results allowed us to compare the performance daily, and annual. These are compared in terms of total height, the configuration of the generator and geographical site. For systems intended for supplying drinking water, the system SP1 which gave the best results.

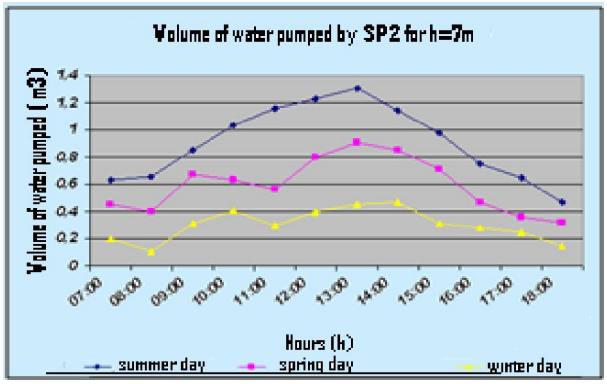

Fig.18. Volume of water pumped daily (spring, summer, winter) with SP2, h = 7m

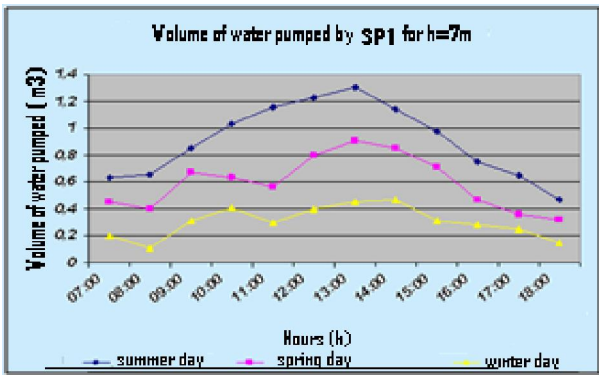

Fig.19 Volume of water pumped daily (spring, summer, winter) by SP1, h =7m .

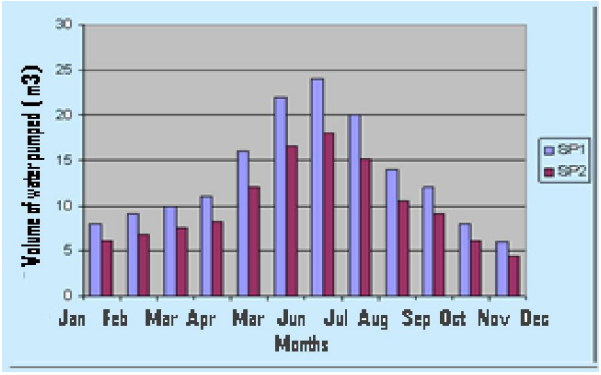

Fig.20 Volume of water pumped annually (2007), h = 7m

REFERENCES

[1] Mohammedi, A., Rekioua, D., Mezzai, N., Experimental study of a PV water pumping system,(2013) *Journal of Electrical Systems* 9 (2) PP. 212 - 222

[2] Rekioua, D., Matagne, E.,Optimization of photovoltaic power systems: Modelization, Simulation and Control,(2012) *Green Energy and Technology* 102

[3] C. Franx, A New Approach to Using Solar Pump Systems Submersible Motors, Proceedings of the 2nd Photovoltaic Solar Energy Conference, pp. 1038 - 1045, 1979.

[4] D.S.H. Chan, J. R. Philips and J.C.H. Phang, A Comparative Study of Extraction Methods for Solar Cell Model Parameters, Solid State Electronics, Vol. 29, No. 3, pp. 329-337, 1986.

[5] L. Keating, D. Mayer, S. McCarthy and GT Wrixon, Concerted Action on Computer Modelling and Simulation, Proceedings of the 10th European Photovoltaic Solar Energy Conference, Lisbon, Portugal, pp. 1259 - 1265, 1991.

[6] Ould-Amrouche, S., Rekioua, D., Hamidat, A., Modelling photovoltaic water pumping systems and evaluation of their CO2 emissions mitigation potential,(2010) Applied Energy 87 (11) PP. 3451 – 3459.

[7] Rekioua, D., Achour, A.Y., Rekiouaa, T., Tracking power photovoltaic system with sliding mode control strategy, (2013) *Energy Procedia* 36 PP. 219 – 230.

.